Journal of the Physical Society of Japan
Vol. 72, No. 12, December, 2003, pp. 3243–3253

ESR Study on the Excited State Energy Spectrum of $SrCu_2(BO_3)_2$ —A Central Role of Multiple-Triplet Bound States—

Hiroyuki NOJIRI, Hiroshi KAGEYAMA[1], Yutaka UEDA[1] and Mitsuhiro MOTOKAWA[2]

Department of Physics, Okayama University, Tsushimanaka 3-1-1, Okayama 700-8530
[1]*Institute for Solid State Physics, University of Tokyo, Kashinoha 5-1-5, Kashiwa, Chiba 277-8581*
[2]*Institute for Materials Research, Tohoku University, Katahira 2-1-1, Sendai 980-8577*

(Received December 19, 2002)

The excited state energy spectrum of a two-dimensional dimer system $SrCu_2(BO_3)_2$ has been investigated by high field ESR. Besides two non-degenerated one-triplet excitations, various types of multiple-triplet bound states are identified: singlet, triplet, and quintet. The intensity of these bound states is extremely strong because one-triplet process is strongly suppressed in the orthogonal dimer system. The bound singlet state is found slightly below the energy gap of the one-triplet state, indicating the proximity to a quantum critical point. A band of the two-triplet bound state splits due to distant neighbor interactions. The bound quintet state is the direct evidence of two-triplet object made up of four $S = 1/2$ spins. The energy of the lowest quintet becomes lower than that of the one-triplet excitation before the closing of the lowest spin gap, namely, the quintet touches first to the ground singlet state. The present investigation exhibits an essential role of multiple-triplet bound states in the magnetic excitation spectrum.

KEYWORDS: $SrCu_2(BO_3)_2$, spin gap, ESR, magnetic excitation, high magnetic field
DOI: 10.1143/JPSJ.72.3243

1. Introduction

Coupled chain and dimer systems have been attracted much attention in this decade. One of the interests is in a complex and fruitful crossover from a well-known purely one-dimensional antiferromagnet to a two-dimensional (2D) antiferromagnet which is the basis of a high-temperature superconductor.[1)] A 2D spin gap system is quite rare, in contrast with a rapid growth of new quasi-one dimensional compounds. One of fundamental difficulties is that a quasi 2D system tends to exhibit three dimensional (3D) long range order. However, the 3D-order is effectively suppressed by introducing frustration. One of the most successful examples is $SrCu_2(BO_3)_2$: a 2D dimer system with considerably strong frustration.[3)]

In this compound, a layer of $S = 1/2$ Cu^{2+} ions is sandwiched by layers of Sr ions in a tetragonal unit cell.[2)] A dimer unit is composed of a neighboring pair of edge-shared planar rectangular CuO_4 and these dimers connect orthogonally by way of a triangular planar BO_3, providing a unique 2D-network as shown in Fig. 1. This 2D lattice is topologically equivalent to a 2D square lattice with additional alternating diagonal interactions, for which the direct product of the singlet pairs is the exact ground state of the system, as proven by Shastry and Sutherland.[4)]

Although the ground state is the unique dimer solid, the excited state is very rich. A low-lying excited triplet, which is dominant for spin gap compounds in general, is considerably suppressed due to the extreme localization.[5)] Higher order multiple-triplet states are instead stabilized by the kinetic energy called "correlated hopping". Those interesting features of the excited state have been studied experimentally and theoretically, although a complete understanding has not been obtained so far.[6–16)]

Another important issue is that the compound is located very close to a quantum critical point. The ratio J_2/J_1 is evaluated to be 0.63–0.68, where J_1 and J_2 are, respectively, the intradimer and interdimer interactions as shown in Fig. 1(a).[17)] The value is just below the critical value of $J_2/J_1 = 0.70$ between the dimer state and the Néel-ordered state. More recently, it has been proposed that a resonating plaquette singlet state exists in between these two states.[18)] The present compound is clearly in the dimer phase. However, a precursor effect of the new ground state may

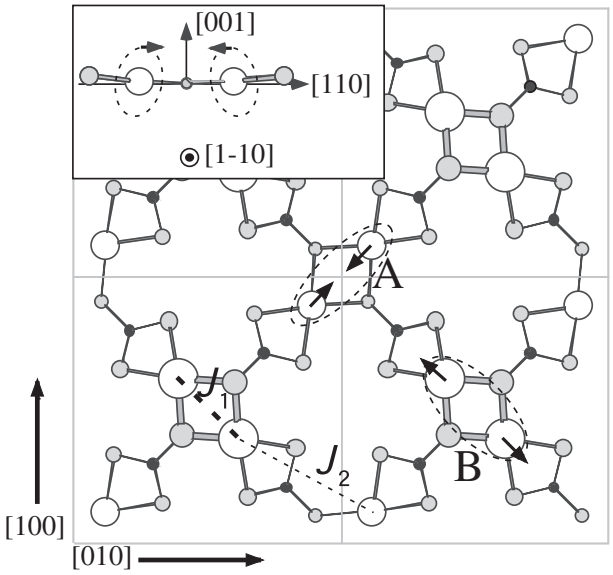

Fig. 1. 2D-dimer plane viewed along the c-axis with respect to $z = 0$, or 0.5. Open, shadowed and closed circles, denotes Cu, O and B ions, respectively. The size of a circle indicates the shift along the c-axis (bigger/smaller, corresponding upward/downward). An arrow on Cu shows a tilting of the principle axis of g-tensor. A and B distinguish two types of dimers (with dashed ellipsoids) which are connected orthogonally each other. Thin square shows a unit cell. J_1 (thick dashed line) and J_2 (thin dashed line) are the nearest neighbor and the next-nearest-neighbor interaction in the plane, respectively. The inset is the [1–10]-axis view of the A-dimer. Ellipsoids schematically represent the anisotropy of g-tensor.

appear in excited states by the proximity to the quantum critical point.

An interesting feature also appears in the magnetization curve with quantized plateaux at one-third, one-quarter and one-eighth of the saturated moment.[19,20] These plateaux are caused by the extreme localization of one-triplet excitation. Namely, the excited triplets cannot propagate freely in the 2D lattice owing to the orthogonal dimer arrangement and consequently organize a regular lattice composed of spatially separated triplets when the density of the triplets is commensurate with the underlying lattice.

As discussed above, it is very interesting to study the excited state spectrum of the present system, especially in high magnetic fields. Among many methods, ESR has established its unique status as a probe of magnetic excitations in high magnetic fields.[21–24] In fact, the one-triplet as well as the multiple-triplet excitations were found in our previous ESR work.[9] However, the richness of the spectrum and the limited frequency range prevented us to complete the experimental determination of a full spectrum. In the present work, a nearly complete excited state energy spectrum up to the two-triplet continuum and up to 40 T is obtained.

The format of the paper is as follows. After briefly mentioning the experimental procedure, we show details of experimental results. The energy diagram, selection rule, and the symmetry of one-triplet and multiple-triplet excitations are examined. The anomalous behavior of the magnetic excitation and its relation to the magnetization around the critical field is discussed in terms of the localization of the bound states.

2. Experimental Procedure

Submillimeter wave ESR measurements have been performed up to 1.3 THz and in pulsed magnetic fields up to 40 T. An optical pumped far-infrared laser, backward-travelling wave tubes and Gunn oscillators have been employed as radiation sources. We have employed a simple transmission method with Faraday configuration where the propagation vector of the incident radiation is aligned parallel to the external magnetic field. The polarization of light is random in the plane normal to the propagation vector. An InSb is used as the detector. The detail of the ESR system is given in the references.[15,25]

High-purity bulk single crystals of $SrCu_2(BO_3)_2$ were grown by the travelling solvent floating zone (TSFZ) method from a polycrystalline $SrCu_2(BO_3)_2$ and a solvent $LiBO_2$ using FZ-T10000N 10 KW high pressure type (Crystal System Inc.) with four halogen lamps as heat sources. Oxygen gas ($P_{O2} = 1$ atom, 99.999%) was being flowed during the growth process.[26] By means of Laue X-ray back-reflection, the grown materials were checked and the crystal axes were determined. A piece of the single crystal with the dimensions of about 4 mm × 4 mm × 1 mm was used for the ESR experiments.

3. One-Triplet Excitation

In the present work, we mainly focus on ESR spectra at 1.6 K and below the critical field H_c at which the gap closes. Since this temperature is much lower than the spin gap, all the signals are assigned to be the excitations from the ground state. In this section, we show important features of an one-triplet excitation: a creation of single triplet in a dimer and we discuss the ESR selection rule considering Dzyaloshinsky–Moriya (DM) interactions and a staggered field. To avoid confusion, we attach subscripts: GS (ground state) and BS (bound state or multiple-triplet excitation), to the terms such as singlets and triplets. For examples, singlet_{GS}, singlet_{BS} and triplet_{BS} represents the singlet ground state, the excited singlet bound state and the triplet bound state, respectively.

3.1 Experimental features

Figure 2(a) shows a typical temperature dependence of ESR spectrum. The intensity of a broad peak at 13.3 T decreases rapidly below 10 K. It indicates that the peak is caused by the transitions of the thermally excited triplets as shown by dotted arrows in the inset. At 1.6 K, two weak signals marked by arrows are observed. Since the intensity of the weak signals increases with decreasing temperature,

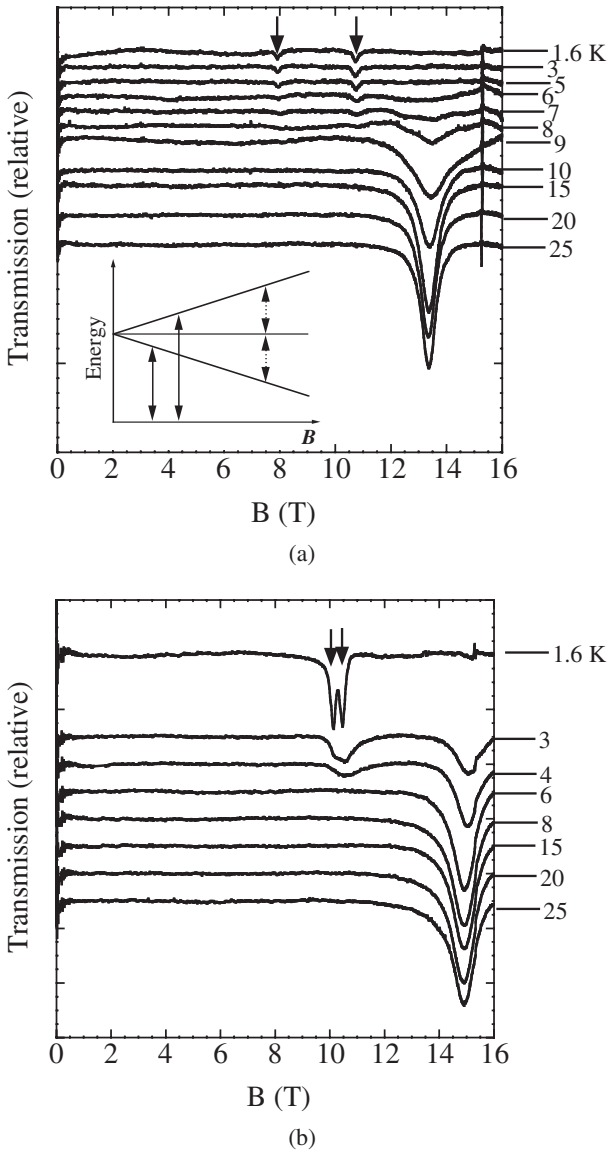

Fig. 2. Temperature dependence of ESR spectra at 428.6 GHz (a) for $\boldsymbol{B} \parallel c$ and (b) for $\boldsymbol{B} \parallel a$. The sharp peak at 15.3 T is the signal of DPPH used as a field maker. The inset shows a schematic energy diagram of triplet with a spin gap.

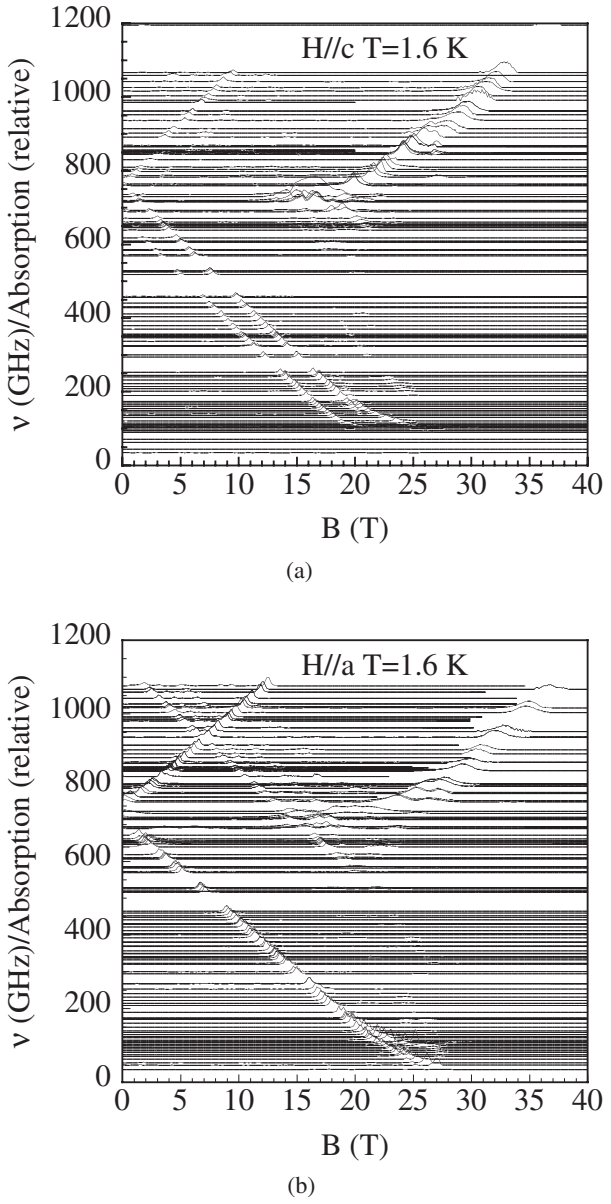

Fig. 3. Summarized magnetic excitation spectra spanning 0–40 T and 0–1100 GHz at 1.6 K, (a) for $\boldsymbol{B} \parallel c$, (b) for $\boldsymbol{B} \parallel a$. To reduce the data volume, the data points are averaged with the interval of 0.1 T.

these are assigned as the transitions between the ground singlet and the excited states, which is indicated by the solid arrows in the inset. While the similar temperature dependence is found for $\boldsymbol{B} \parallel a$ in Fig. 2(b), differences are found in the splitting and the intensity of the two peaks. As is well known, an ESR transition between the ground singlet and the excited triplet states due to the mechanism of magnetic dipolar transition is usually forbidden.[27] A non-secular term such as DM-interaction, as proposed recently by Cépas *et al.*, may be the leading origin of the break down of the selection rule.[16] This point will be discussed later.

In Figs. 3(a) and 3(b), ESR spectra measured at different frequencies are collected together for $\boldsymbol{B} \parallel c$ and $\boldsymbol{B} \parallel a$, respectively. In these figures, each ESR spectrum is plotted in such way that its background coincides with the measured frequency, so that the resultant plot can be regarded as a kind of the frequency–field diagram which furthermore show intensity variation of excitations. A detailed frequency field diagram is obtained by tracing different types of peaks in the plot. Frequency–field diagrams thus obtained are depicted in Figs. 4(a) and 4(b) for $\boldsymbol{B} \parallel c$ and for $\boldsymbol{B} \parallel a$, respectively. A contour map of the intensity in the frequency–field plane is shown in Fig. 5. Those figures are useful to see the overview of the excited state energy spectra in field–frequency plane. A complicated structure of the spectrum is noticed, that cannot be expressed well by a simple frequency–field plot. In the following, we show important features of the one-triplet excitation using the set of these figures.

In Figs. 4(a) and 4(b), it is noticed that two low-lying triplet excitations: O_1 and O_2 exist. The values of the zero field gaps are close to the spin gap estimated from magnetic susceptibility and high field magnetization;[3,19] hence these modes are assigned as one-triplet excitation. More precisely, the zero field energy gaps of O_1 and O_2 are 764 ± 2 GHz and 679 ± 2 GHz, respectively for $\boldsymbol{B} \parallel c$. The splitting between O_1 and O_2 is largest in this direction. The spin gap E_g is determined to be 722 ± 2 GHz, which is evaluated as the average of the zero field intercepts of O_1 and O_2. The existence of two modes is generally expected when a unit cell contains two magnetic ions. The two modes, originally degenerated, may be split by an anisotropic inter-dimer interaction and/or other perturbations. In the present compound, the splitting of the two-modes is interpreted fairly well by including a inter-dimer DM-interaction.[16]

When a magnetic field is rotated from the ***c***-axis to the ***a***-axis, the splitting shows a monotonic decrease and takes a non-zero minimum for $\boldsymbol{B} \parallel a$ as we reported in the previous work (see Fig. 4 of ref. 9). The angular dependence of the upper-going branches of O_1 and O_2 is more clearly shown in Fig. 6. The two modes are almost parallel to each other for $\boldsymbol{B} \parallel c$, while they become very close each other for $\boldsymbol{B} \parallel a$ accompanied by the bending around zero field. The behavior indicates that the principle axis of the interaction causing the splitting points to the ***c***-axis.

It should be stressed here that a small but intrinsic splitting exists between O_1 and O_2 for $\boldsymbol{B} \parallel a$. It should be noted that the splitting is not caused by the sample misorientation or anisotropy of g-value. This can be partly confirmed if one measures the two modes for $\boldsymbol{B} \parallel [110]$. In this case, as shown in Fig. 1, the magnetic field is parallel to the A-dimers and is perpendicular to the B-dimers. A larger splitting would be expected, if it was caused by the difference of g-value between the A-dimer and B-dimer. However, it is found that the splitting is nearly identical with that for $\boldsymbol{B} \parallel a$ (not shown here). The result indicates that the small splitting observed for $\boldsymbol{B} \parallel a$ is not caused by the g-value anisotropy.

The essential difference between O_1 and O_2 in $\boldsymbol{B} \parallel a$ is found in the mixing behaviors as follows. Firstly, it is found that the magnitude of the mixing with singlet_{BS} states is different between O_1 and O_2. In Fig. 4(b), O_1 shows a break around 860 GHz, while O_2 shows another break around 650 GHz. These breaks may be caused by an anti-level-crossing with an excited singlet state (this point will be discussed later). Secondly, it is noticed that O_1 and O_2 round very differently around H_c where a mixing with the ground state occurs. A mixing is strongly related to the symmetry of corresponding modes; hence these findings indicate that the symmetry of O_1 is different from that of O_2.

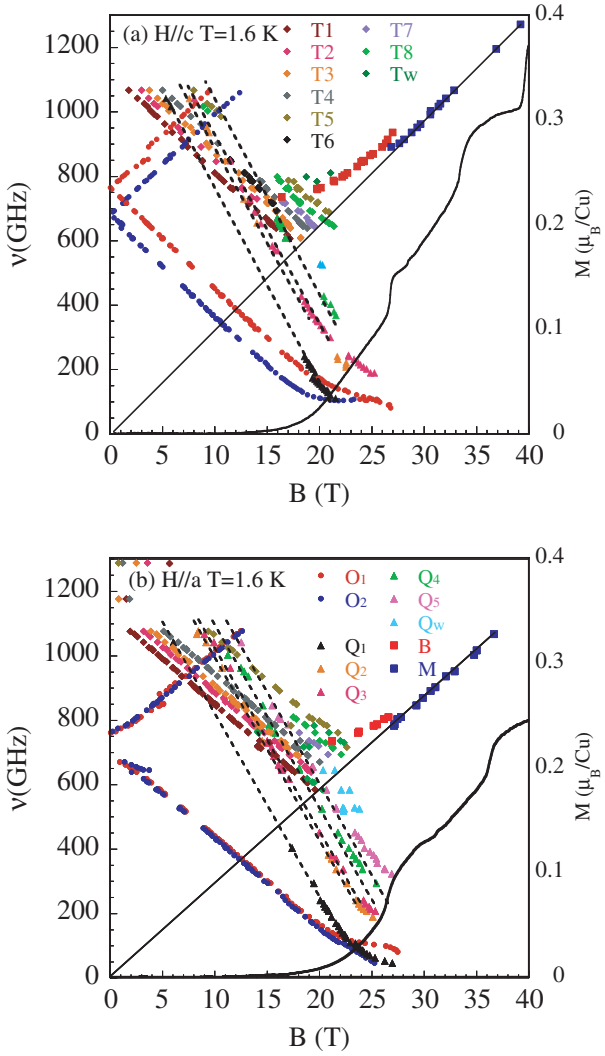

Fig. 4. Frequency–field diagram at 1.6 K (a) for $\boldsymbol{B} \parallel c$ and (b) for $\boldsymbol{B} \parallel a$. O, T, Q, B, M are one-triplet, triplet$_{BS}$, quintet$_{BS}$, new signal and paramagnetic like signal, respectively. For details, see text. The subscript W denotes weak signals which are not well classified. Solid line shows the paramagnetic resonance line ($\nu = g\mu_B H$, ν: frequency, g: g-value). Dashed lines are eye guides. Magnetization curves taken from ref. 20 are plotted together.

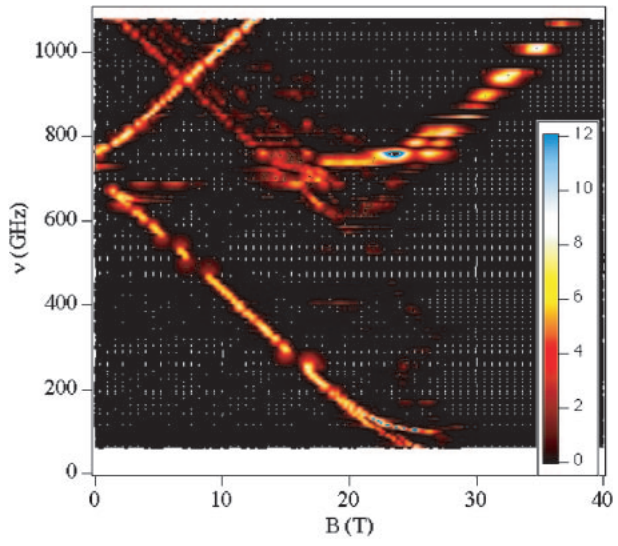

Fig. 5. Contour plot of ESR absorption intensity for $\boldsymbol{B} \parallel a$ at 1.6 K. The color scale is arbitrary.

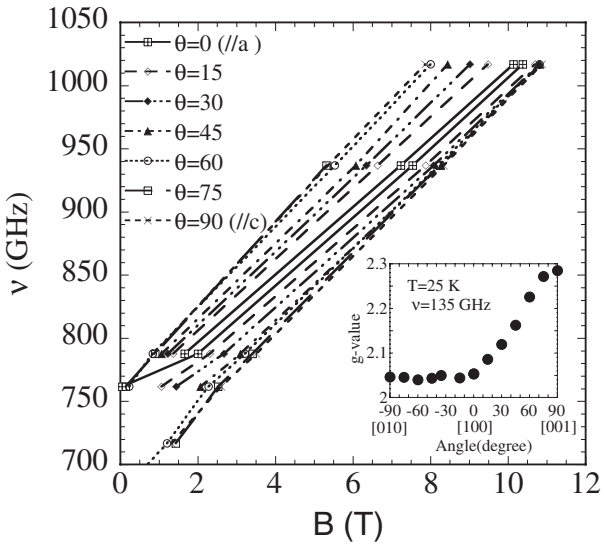

Fig. 6. Angular dependence of O_1 and O_2 in the ac-plane. θ is the angle between the a-axis and an external field. Lines are eye-guides. Anisotropy of g-value is plotted in the inset, which is measured at 25 K with 135 GHz. The negative angle corresponds to the rotation of an external field from the a-axis to the b-axis.

Next we discuss the intensity of the one-triplet excitation. For $\boldsymbol{B} \parallel c$, a clear difference is found in the field dependence of intensity between O_1 and O_2 as shown in Fig. 3(a). The intensity is nearly field independent for O_1, while it is sensitive to the magnetic field intensity for O_2. Namely, the intensity of the down-going branch of O_2 increases with increasing field and that of the up-going branch decreases with increasing field. In addition to this, a rapid decrease of intensity is observed for O_2 around zero field. The behavior suggests that the origin of the break down of the selection rule is different between O_1 and O_2.

In $\boldsymbol{B} \parallel a$, the behavior is much different from that in $\boldsymbol{B} \parallel c$. First, the intensity is nearly field independent for both O_1 and O_2. Secondly, the intensity is stronger than that in $\boldsymbol{B} \parallel c$. The second feature suggests that a non-secular term causing these transitions should be larger for $\boldsymbol{B} \parallel a$.

We compare the present result with that of the FIR spectroscopy.[12] It should be reminded that the definitions of absorption intensity are not exactly same each other. In our case, the intensity is normalized by the intensity of DPPH used as maker or by the intensity of paramagnetic signal. In the FIR experiment, the magnetic intensity is obtained by taking a difference between a high temperature spectrum and a low temperature one. In spite of this difference, two results are roughly consistent each other. In Fig. 4 of ref. 12, a field is applied along the a-axis. The intensity decreases with increasing field for the c-polarization, while it increases for the ab-polarization. In case of ESR, un-polarized radiation is used and thus the intensity should be averaged over the two polarizations. If we average the data of different polarizations obtained by FIR spectroscopy, it can happen that the intensity depends on magnetic field only weakly for the cancellation, which agrees with the ESR result for $\boldsymbol{B} \parallel a$.

3.2 Selection rule and DM-interaction

In the following, we discuss possible interactions allowing the finite intensity of the one-triplet excitations, which is

originally forbidden. We consider an intra-dimer DM-interaction: $\boldsymbol{D}_d$, the c-axis and the ab-plane components of inter-dimer DM-interaction: ($\boldsymbol{D}_c$ and $\boldsymbol{D}_{ab}$, respectively) and a staggered field, all of which are allowed to exist by its crystal structure. We do not consider a novel mechanism: dynamical DM-interaction proposed recently.[28,29] Now the point to be clarified is what aspect of the experimental result can be interpreted with those four terms. We would refuse to deny or confirm the existence of the dynamical DM-interaction because the judgement cannot be made with present experimental results.

We employ the selection rule established by Sakai, Cépas and Ziman for DM-interaction.[27] Since the present experiment is made in Faraday configuration, one simple rule is applicable as follows.

DM-rule: *Field independent intensity is observed only when the DM-interaction has a component along the external magnetic field and the intensity is quadratic to the component.*

Among three possible DM-interactions, $\boldsymbol{D}_c$ exists irrespective of the small buckling of the edge-shared CuO_4 planes as shown in Fig. 1. $\boldsymbol{D}_d$ and $\boldsymbol{D}_{ab}$ exist only when this buckling is taken into account. A staggered field becomes also possible for the buckling as shown in the inset of Fig. 1. Considering the large anisotropy of g-value in the ac-plane ($g_a = 2.05$ and $g_c = 2.28$) and the small one in the ab-plane ($\Delta g \leq 0.01$, see Fig. 6 inset), a sizable staggered field is expected only for $\boldsymbol{B} \parallel c$. Those three terms caused by the buckling may be small, because of the small tilting angle. An experimental estimate of $\boldsymbol{D}_{ab}$ is made by Kakurai *et al.*[30] and it is found that the magnitude of $\boldsymbol{D}_{ab}$ is about 30% of that of $\boldsymbol{D}_c$. This value looks overestimated since the buckling angle is quite small. However, it is important that the practical effect is observed with such small buckling. One should consider even a small $\boldsymbol{D}_c$ because it operates directly on the two spins in a dimer. From the crystal symmetry it is evident that $\boldsymbol{D}_d$ lays in the ab-plane. The direction is perpendicular to a dimer bond. Since two kinds of dimers are orthogonally arranged in the ab-plane, the sum of the squares of a field-parallel-component of $\boldsymbol{D}_d$ over the A-dimers and the B-dimers is constant for any field direction in the plane.

Let us examine, if the DM-rule is compatible with the experimental results. Considering the DM-rule, $\boldsymbol{D}_c$ gives rise to constant ESR intensity for $\boldsymbol{B} \parallel c$. This expectation is consistent with the behavior of O_1 in which the intensity is field-independent. A precise estimation of $\boldsymbol{D}_c = 0.18\,\mathrm{meV}$ is made from the dispersion measured by neutron scattering.[16] This value is a standard when we estimate the magnitude of DM-interaction from the ESR intensities.

Contrary to O_1, the field dependence of the intensity of O_2 is not compatible with the DM-rule and thus DM-interaction is not the origin of the transition O_2. As shown in the previous section, the intensity of O_2 shows the characteristic field dependence. It is noticed that the behavior is similar to the case of a staggered field with Voight configuration.[31] In fact, a staggered field is expected for this field orientation as mentioned above. However, it cannot be applicable to the present experiment because the Faraday configuration is used. It is clear that neither DM interaction nor a staggered field can cause the transition O_2 in the lowest order. A possibility is that a combined higher order term may cause a finite ESR intensity. The fact that the intensity of O_2 is much weaker than that of O_1 is consistent with the contribution of the higher order term. A similar situation is found in $CuGeO_3$, in which both optical and acoustic branches are observed in ESR. This behavior also cannot be interpreted by the lowest order term of DM-interaction.[27] As discussed above, it is rather plausible that a combined higher order term of DM interaction and a staggered field causes the transition O_2. A theoretical calculation of the intensity is necessary to clarify the present proposal.

Next we discuss the case of $\boldsymbol{B} \parallel a$. Since both $\boldsymbol{D}_d$ and $\boldsymbol{D}_{ab}$ have the field parallel components, the field independent intensity observed in the experiment is compatible with the DM-rule. The fact the intensity is larger in $\boldsymbol{B} \parallel a$ than that in $\boldsymbol{B} \parallel c$ indicates that the field parallel DM-component is larger in $\boldsymbol{B} \parallel a$. However, the square of the magnitude of $\boldsymbol{D}_{ab}$ is one-order smaller than that of $\boldsymbol{D}_c$; hence $\boldsymbol{D}_{ab}$ causes the minor contribution to the intensity and $\boldsymbol{D}_d$ should be dominant in $\boldsymbol{B} \parallel a$. Another piece of the evidence of the major contribution of $\boldsymbol{D}_d$ is that the intensity of O_1 and O_2 is almost constant when we rotate an external magnetic field within the ab-plane (not shown here). It is consistent with the fact that the sum of the squares of the field parallel components of $\boldsymbol{D}_d$ over A- and B-dimers is constant under this field rotation. Moreover, $\boldsymbol{D}_d$ operates directly on each dimer, while $\boldsymbol{D}_{ab}$ does not. All these facts indicate that the $\boldsymbol{D}_d$ is the main cause of the selection rule breaking in $\boldsymbol{B} \parallel a$.

Finally, we would like to make a comment on an exchange anisotropy. In our previous work, we did not consider the inter-dimer DM-interaction and mentioned that exchange anisotropy may cause the splitting between O_1 and O_2 and the forbidden transitions. Recent proposal by Cépas *et al.* that DM-interaction is the leading term is more plausible than the exchange anisotropy. Now we consider that a simple exchange anisotropy term does not cause the mixing between the singlet ground and the excited triplet states. However, a consideration of the problem from more general view point may be interesting.[2,32,33] High resolution of ESR can resolve even a small change of triplet excitation caused by these terms.

4. Multiple-Triplet Bound States

As shown in Figs. 3(a) and 3(b), many high energy excitations: multiple-triplet bound states,[15] account for a considerable weight in the excited state. In the present system, a sizable inter-dimer interaction exists. This interaction couples two (or three) triplets on dimers and causes a bound sate with total spin $S = 2$ (or $S = 3$). A $S = 2$ bound state, for example, consists of three sub-states; singlet, triplet and quintet. Usually such bound state appears as a continuum. In an orthogonal-dimer system, however, the localization of triplets causes the discrete states. In this section, we describe the behaviors of those bound state excitations in detail.

4.1 Singlet bound state

A $\mathrm{singlet}_{BS}$ is an excited singlet state consisting of two interacting triplets on nearby dimers and the energy is given by subtracting the binding energy from the twice of E_g. For a frustrated spin gap system, it is expected theoretically that

excited singlets can dominate the states below E_g. In highly frustrated system, an excited singlet lies in the low energy range close to the ground state. In another word, the magnitude of the binding energy is a yardstick for the degree of frustration. In the present case, such a low energy excited singlet indicates the close distance from a quantum critical point.

A singlet$_{BS}$ is observed through the anti-level-crossing with one-triplet excitation as shown in Figs. 7(a) and 7(b). In Fig. 7(a), as the frequency increases toward 646 GHz, O_2 deviates from O_1 and shifts to the low-field side with a considerable broadening. Above this frequency, O_2 approaches to O_1 from the high-field side. For O_1, a conventional successive Zeeman shift is found. The bending of O_1 around zero field is caused by the anisotropic inter-dimer DM-interaction as discussed in the previous section. The break of O_2 shown in Figs. 7(a) and 3(b) is a typical behavior of an anti-level-crossing. Although the singlet$_{BS}$ cannot be observed directly by ESR, the anti-level-crossing exhibits clearly the existence of the singlet state TS_1 at 646 GHz. A similar anti-level-crossing is found at 860 GHz between the singlet TS_2 and O_1 as shown in Fig. 7(b). When the frequency is very close to TS_2, O_1 disappears and only a single peak of O_2 is found. The magnitude of the anti-level-crossing at TS_2 is larger than that at TS_1. It indicates that the coupling between the singlet$_{BS}$ and the one-triplet state is larger in TS_2.

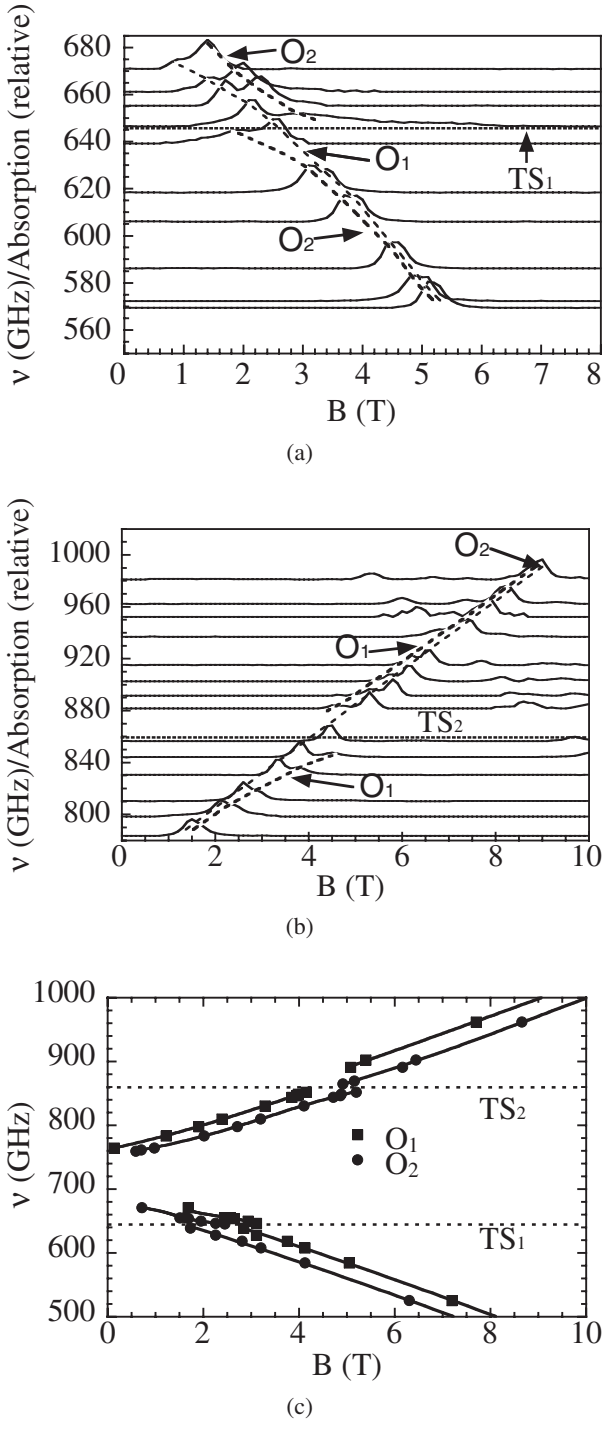

Fig. 7. (a) ESR spectra around the anti-level-crossing between O_2 and TS_1 (dotted line). Dashed lines are eye-guides. (b) Same for O_1 and TS_2 (dotted line). (c) Frequency–field diagram at 1.6 K, where an applied magnetic field is tilted 15° from the *a*-axis in the *ac*-plane. Dashed lines are eye-guides.

The present result also exhibits that the symmetry of the one-triplet excitations O_1 and O_2 are different each other as mentioned in the previous section. In Fig. 7(c), a frequency–field diagram is plotted, where a magnetic field is in the *ac*-plane but not parallel to the *a*- nor the *c*-axes. An anti-level-crossing is found in both O_1 and O_2 at both TS_1 and TS_2 (four breaks in total). This behavior shows that two-modes O_1 and O_2 are mixed each other when an external field is tilted from the principle-axes (*a* or *c*) of the crystal. It implies that the anti-level-crossing is closely related to the anisotropic part of exchange coupling such as DM-interaction.

Let us compare the present results with the Raman scattering experiments, where several singlet bound states are found.[8] A clear peak was observed at 30 cm^{-1} (900 GHz) in B_1 polarization (see Fig. 1 of ref. 8). In B_2 polarization, a peak was also found at 30 cm^{-1} with a shoulder at 24 cm^{-1} (720 GHz). The shoulder appeared also in B_1 polarization and a small low energy shift was found at 6 T. Consequently, the shoulder was assigned as one-triplet excitation being weakly allowed for some defects. The energy of TS_2 is very close to 30 cm^{-1} and thus TS_2 can attribute to the 30 cm^{-1} Raman peak. For TS_1, no corresponding Raman peak exists; hence TS_1 located at 646 GHz (21.5 cm^{-1}) is assigned as the lowest singlet bound state. It is notable that the energy is lower than the spin gap of the one-triplet excitation. This fact indicates that the system is rather close to the quantum critical point where the energy of the bound state should fall to zero.

Let us compare the present results with the theoretical investigations on various bound states.[10,14,35] As discussed by Totsuka, Miyahara and Ueda, the representations *E* and B_2 are infrared (also ESR) active and those A_2 and B_1 are infrared inactive in D_{2d} symmetry. The one-triplet belongs to the *E* representation. In ref. 35, the lowest singlet$_{BS}$ is found to have the $A_2 \otimes B_1$ symmetry (additional small splitting is found in ref. 14). The second lowest singlet$_{BS}$ coming from the third neighbor pair in ref. 35 has an infrared active $A_1 \otimes B_2$ symmetry. Let us assign tentatively the lowest energy mode and the second lowest energy mode to TS_1 and to TS_2, respectively. It is natural to assume that the one-triplet shows the stronger mixing with the infrared active mode. The strong/weak anti-level-crossings of TS_2/TS_1 are consistent

with the fact that the lower singlet$_{BS}$ (TS_1) is infrared inactive and that the upper one (TS_2) is infrared active. However, since only two modes are found in the present experiments, the definite assignment is difficult. A theoretical investigation by considering the mixing effect is needed for further understanding. Such a calculation is useful to examine the wave function of the bound states.

4.2 Triplet bound state

In Fig. 8, an example of ESR spectrum is shown for $\boldsymbol{B} \parallel a$. Besides one-triplet excitations O_1 and O_2, eight peaks are found. These additional peaks are easily classified into triplets$_{BS}$ (T_1–T_5) and quintets$_{BS}$ (Q_1–Q_3) by Zeeman shifts in the frequency–field diagram. In the inset of Fig. 8, temperature dependence of intensity is plotted for different peaks. Below 7 K, the intensity increases with decreasing temperature with similar temperature dependence for all three peaks. The behavior confirms that the additional peaks are the excitations from the ground state.

A most significant feature in Fig. 8 is the sizable intensity of the bound state excitations. It is the evidence of the large suppression of the one-triplet process in the present system. It also supports the idea that a bound state propagating with correlated motion has considerable spectral weight.[35] In general, ESR intensity is not a spectral weight itself because it is mediated by transition matrix elements. However, the intensity can be compared directly between the one-triplet state and the triplet$_{BS}$. The argument is based on the fact that a total spin number of the system changes by one in both types of excitations. From this basic view point, we notice that the magnitude of matrix element may not be so different (at least in the same order) between these two processes. In fact, the intensity ratio of the sum of O_1 and O_2 to T_1 is comparable with that of the first excited peak to the second one in neutron scattering (see Fig. 4 of ref. 16).[16] This fact supports our presumption that relative ESR intensity of the triplet states (in both the one-triplet and the bound state) roughly corresponds to the difference in the spectral weight.

Another important finding is that the bound state spectrum splits into many sharp discrete peaks instead of a conventional two-triplet continuum. It suggests that many different types of bound state is formed for different interactions acting between the distant triplets on dimers. The fact that these different states do not merge into a single band suggests that the dispersion of the bound states is very weak.

Let us evaluate the zero field energy gap of each bound state. We simply evaluate a gap by extrapolating each mode with a linear equation. This procedure may cause non-negligible error, if the level of a bound state has a large bending around zero field as is observed in O_1 and O_2. To check this point, we compare a zero field gap obtained for $\boldsymbol{B} \parallel a$ with that for $\boldsymbol{B} \parallel c$ and found that the difference is at most 10 GHz. It is much smaller than that of O_1 and O_2 ($\sim$40 GHz) and is comparable with experimental errors. Hence, the above mentioned procedure is justified. The energy gaps of the bound states thus evaluated are listed in Table I. We speculate that the anisotropy of the zero field splittings of the bound states are reduced effectively by the hopping effect or by the spread of the wave function over distant dimers. Another finding is that the anisotropy of the intensity of the triplets$_{BS}$ except T_1 is similar to that of the one-triplet excitations. It shows that the origin of the break down of the selection rule may be the same for both cases.

Next we discuss ESR spectra around the one-triplet gap as shown in Figs. 9(a) and 9(b). The spectra change drastically both in the shifts and in the intensity in the tiny range of frequency. This behavior may be caused by the increasing mixing between the triplet$_{BS}$ and the one-triplet state. Most spectacular feature is found at 736.1 GHz for both $\boldsymbol{B} \parallel a$ and $\boldsymbol{B} \parallel c$. A broad and intense peak consists of many different sub-peaks is found in high field side. Since the anomaly is found at the identical frequency irrespective of field direction, it may be caused by the mixing with a horizontal level lying at this particular energy. Considering the no-mixing of the triplet$_{BS}$ with TS_2 [no break is found in Figs. 4(a) and 4(b)] and the no-mixing of the one-triplet states with the new horizontal level, it may not be a singlet bound state. The $S_z = 0$ branch of the one-triplet at zero wave vector point is located at 722 GHz and it cannot be the candidate of the new singlet state. It is noticed that an $S_z = 0$ branch of the one-triplet at the (1.5, 0, 0) point is found exactly at this energy by neutron scattering (see Fig. 3 of ref. 30). This $S_z = 0$ branch may be responsible for the

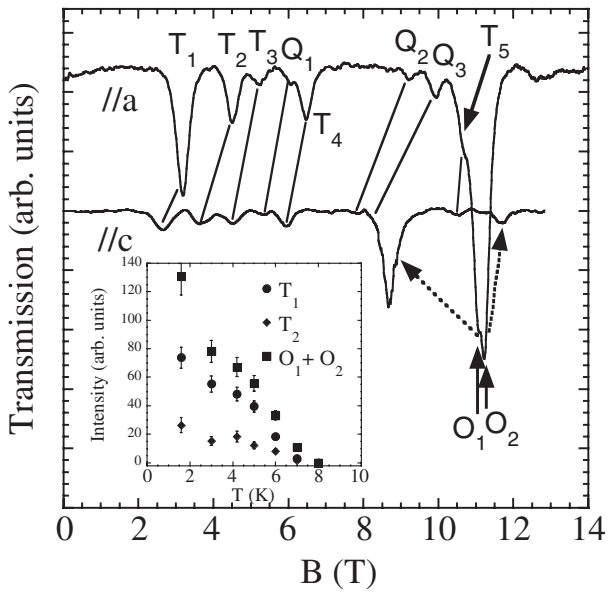

Fig. 8. Anisotropy of ESR spectrum at 1024 GHz and at 1.6 K. Dotted arrows indicate the splitting of O_1 and O_2. Lines connect corresponding peaks. Temperature dependence of intensity is shown in the inset. See text for the notation of peaks.

Table I. Zero field energy gap of the bound states. The notation is identical to that in Figs. 4(a) and 4(b).

Triplet	Gap (GHz)	Quintet	Gap (GHz)
T_1	1140 ± 5	Q_1	1390 ± 15
T_2	1170 ± 5	Q_2	1560 ± 15
T_3	1190 ± 5	Q_3	1600 ± 15
T_4	1225 ± 5	Q_4	1652 ± 15
T_5	1350 ± 5	Q_5	1729 ± 15
T_6	1220 ± 5		
T_7	1264 ± 5		
T_8	1303 ± 5		

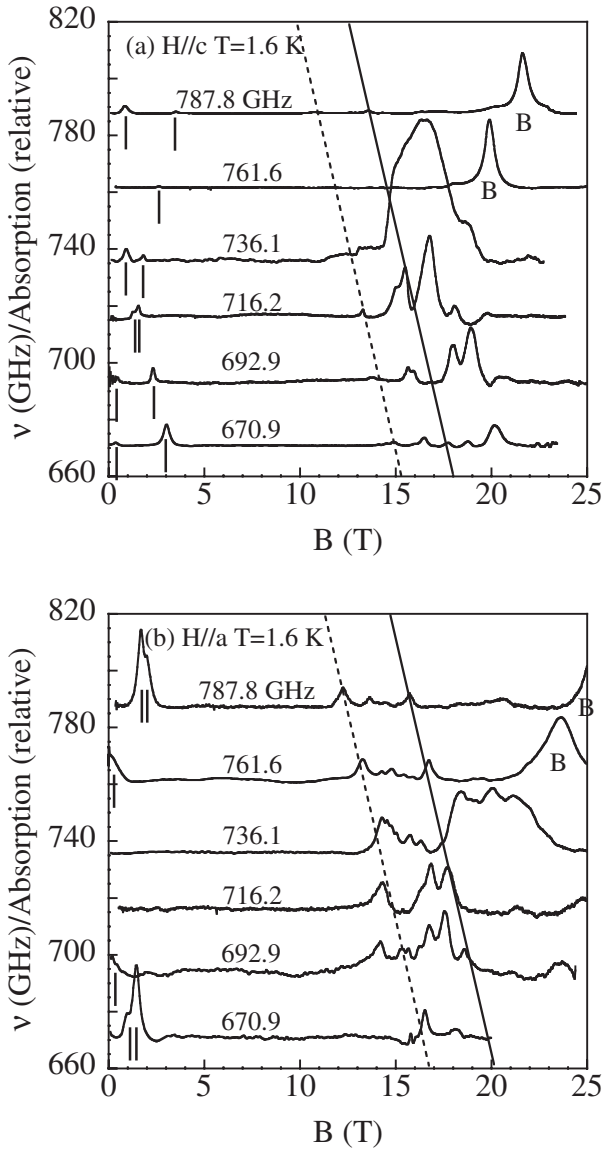

Fig. 9. ESR spectra around the one-triplet gap at 1.6 K (a) for $\boldsymbol{B} \parallel c$ and (b) for $\boldsymbol{B} \parallel a$. Dashed and solid lines are guides of T_1 and T_4, respectively. Vertical bars show O_1 and O_2. B is a peak appearing around H_c.

anomaly at 736.1 GHz. Such mixing between the excitation at zero-wave vector points [(0, 0, 0) and equivalent points] and that at π-wave vector point such as (1.5, 0, 0) is possible by some non-secular terms such as a staggered field. Weaker but similar anomalies are found in Fig. 5 as horizontal high intensity lines, which may be caused by the similar origin.

Let us compare the present results with theoretical calculations. As shown in Table I, all eight bound sates are below the bottom of the two-triplet continuum ($2E_g =$ 1444 GHz) and thus these states are stable as a two-triplet bound state. In ref. 35, only five modes (reducing to three with degeneracy) are found below the bottom. All the mode are infrared active and thus we can attribute at least the five from the all eight modes to the theoretical ones. In the exact diagonalization result which is more reliable around a quantum critical point, two peaks are found side by side around 5 meV (1208 GHz). The energy is close to those of T_1 and T_2. In other theoretical works, the number of states is also less than that found in the present experiment.[10,14] To have more bound states in calculation, the interactions between distant dimers should be taken into account (an inter-layer coupling may also contribute). Finally we mention the instability of a triplet$_{BS}$ due to the transition to another ground state, proposed in theoretical work.[10] In spite of detailed experiments, no such anomalous behavior is found in the present work.

4.3 Quintet bound state

In the following, we show the first observation of a quintet$_{BS}$ in this compound. The nature of the magnetization appearing around the H_c is also discussed.

As shown in Fig. 8, the intensity of a quintet$_{BS}$ is weaker by one order of magnitude than that of triplet$_{BS}$. It is because of the higher order excitation process of the total spin change: $\Delta S = 2$. Five quintet$_{BS}$ modes are found easily for the typical double Zeeman shift. The zero energy gap of quintet$_{BS}$ has been extrapolated from the experimental data. Since the number of data points is limited, the error of the gap is about 15 GHz as listed in Table I. The anisotropy of the gap is not found within the experimental error.

It is notable that only Q_1 is below the two-triplet continuum threshold starting at $2E_g = 1444$ GHz, while the other four modes are located above the threshold. Since the energy of Q_1 is below the threshold, it is assigned as a quintet$_{BS}$ made up of two-triplets (four spins). Let us discuss the nature of other high energy quintets$_{BS}$. In the isolated dimer limit of four spins, the triplet$_{BS}$ and quintet$_{BS}$ are separated by the effective antiferromagnetic interaction acting among the four spins. In this limit, the higher energy of Q_2–Q_5 can attribute to this interaction and those peaks are considered as two-triplet bound state. This interpretation has a difficulty because a multi-particle bound state is unstable when the energy is above the corresponding incoherent continuum in general. It is totally unclear if the quintet sector of the bound state can separate clearly from the continuum spreading above $2E_g$. A more natural idea is to assign Q_2–Q_5 to three-triplet bound state and in fact such three triplet state is found in theoretical calculations, which is shown in later. The existence of three-triplet bound state shows the significant contribution of higher order excitations.

The existence of Q_1 below the threshold causes the peculiar feature that the quintet$_{BS}$ touches the ground state before the closing of one-triplet gap. In spite that a finite mixing between the ground and excited states modifies this simple situation to the more complex one, a characteristic contribution of a quintet is found experimentally. The enlarged spectra of Figs. 4(a) and 4(b) around the H_c are shown in Figs. 10(a) and 10(b). It is noticed that ESR modes bend around the H_c and the behavior is much different between $\boldsymbol{B} \parallel c$ and $\boldsymbol{B} \parallel a$. This anisotropy of ESR spectra should correspond to the anisotropy of the magnetization curves. It is because the magnetization around the H_c is caused by the mixing between the ground and the excited states. In another word, the magnetization should be dominated by the wave function component of the modes enhanced by the mixing. Keeping this point in mind, let us examine the magnetization and the frequency–field diagram carefully.

For $\boldsymbol{B} \parallel c$, the magnetization becomes finite above 15 T

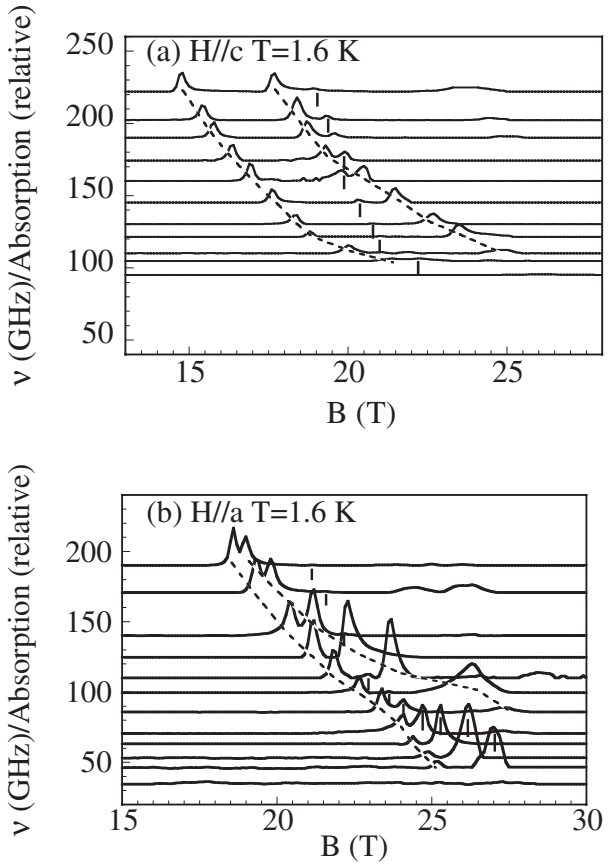

Fig. 10. The low energy part of ESR spectra around H_c (a) for $\boldsymbol{B} \parallel c$ and (b) for $\boldsymbol{B} \parallel a$. The dashed lines are eye-guides. The vertical bar denotes Q_1.

and at the same time O_2 starts to deviate from a straight line. This fact shows that the one-triplet component dominates the magnetization. The intensity of Q_1 is enhanced around 20 T presumably for the weak anti-level-crossing with O_1. Around 21 T, Q_1 disappears and this fact indicates that the quintet component in the magnetization is small. After the anti-level-crossing, O_1 bends considerably and loses the intensity gradually. It is noticed that O_2 shows a turn around like behavior above 20 T, which indicates the strong mixing with the ground state. On the other hand O_1 goes down again above 26 T and disappears suddenly at the jump of magnetization to the 1/8-plateau as shown in Fig. 4(a). The origin of the flat part of O_1 around 25 T might be a anti-level-crossing with a new singlet$_{BS}$, however, a further investigation is necessary for this point.

The strong mixing of O_2 with the ground state indicates the dominant contribution of the one-triplet component to the magnetization. It is also noticed that Q_3 is enhanced with a large rounding above 20 T, which shows the mixing of three-triplet state with the ground state. The contribution of different components to the magnetization indicates that the magnetization is not uniform and homogeneous. It is much different from a usual spin gap system in which a magnetization consists of homogeneously distributed triplets. This characteristic behavior may be caused by the localization of excited states in the present system. Recently, a homogeneous internal field is found by NMR below the 1/8-plateau, however the difference is presumably due to the low observation frequency in NMR, in which the distribution of an internal field is averaged.[38)]

Let us discuss the case of $\boldsymbol{B} \parallel a$ shown in Fig. 10(b). While the behavior of O_1 is similar to that in $\boldsymbol{B} \parallel c$, both Q_1 and O_2 continuously go down toward the ground state. The enhancement of Q_1 and the disappearance of O_2 indicates that the quintet$_{BS}$ component dominates the magnetization. Other higher energy quintet$_{BS}$ states also exhibit enhancements and bendings, which indicate the strong mixing of the quintets$_{BS}$ with the ground state. An observation of a small break of O_2 in $\boldsymbol{B} \parallel a$ [see Fig. 4(b)] and at 22 T may be caused by the anti-level-crossing with unknown singlet$_{BS}$ at 100 GHz, which is also found in $\boldsymbol{B} \parallel c$.

As shown above, the magnetization below the 1/8-plateau contains different types of states and does not consist of homogeneously distributed triplets. A dominant contribution of a quintet$_{BS}$ is found for $\boldsymbol{B} \parallel a$. It is an interesting point, if a quintet$_{BS}$ coupled by an effective repulsive interaction shows a condensation at H_c as proposed by Momoi and Totuska.[13)] Experimentally the domination of the quintet$_{BS}$ is found clearly in the present work. However, it may be a quenched and localized state rather than a condensation. In the case of a condensation, a magnetization should not contains a several different states as observed in the present case. The localization of excited states and the resulting heavy effective mass of a quintet$_{BS}$ may prevent the condensation of quintet$_{BS}$.

Finally we compare the present results with the theoretical calculation of the quintet$_{BS}$. In ref. 35, the lowest mode has the $A_2 \otimes B_1$ symmetry, which is infrared inactive. Since a quintet$_{BS}$ shows very weak intensity, an infrared inactive mode should not be excluded from the candidate. The fact that the number of two-triplet quintet$_{BS}$ is only a few is consistent with the present result. However, a large number of a three-triplet quintet$_{BS}$ found in the experiment calls for further theoretical investigations.

5. High Field Phase

In this section, we discuss ESR signals observed above H_c and their concerns with the magnetization plateaux. In this region of magnetic field, the most of the intensity concentrates into the signals B and M as shown in Figs. 3(a) and 3(b). These two signals alternate at the magnetization jump to the 1/8-plateau as shown in Fig. 11. The position of M is identical with that of the corresponding paramagnetic resonance and the extrapolation of M crosses the origin of the frequency–field diagram for both $\boldsymbol{B} \parallel c$ and $\boldsymbol{B} \parallel a$ as shown in Figs. 4(a) and 4(b). On the other hand, B shows the asymptotic behavior to the paramagnetic line. When a spin gap is closed, a 3D ordered-state or a disordered ground state consists of gap-less triplets appears. In the former, a field variation of a spin wave mode is observed as an antiferromagnetic resonance (AFMR). In the latter, the Zeeman splitting of a gapless triplet causes ESR at the identical resonance field with that of paramagnetic resonance. The strong correlation among the spins does not cause a shift of resonance field because the spin operator commutes with the isotropic exchange coupling.[39)]

The behavior of M shows that the signal is the ESR of a disordered state. It is noticed that M continues at 1/4-plateau and a gapped low-energy excitation is absent. Such low energy discrete excitation is observed at 1/3-plateau, which

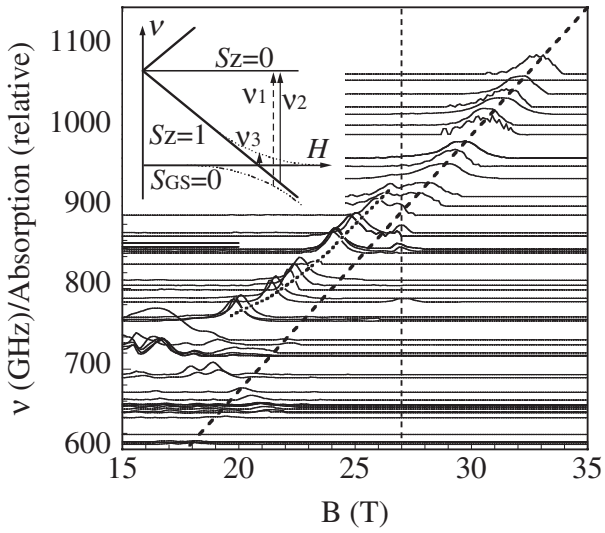

Fig. 11. The ESR spectra around the 1/8-plateau for $\boldsymbol{B} \parallel c$ at 1.6 K. The thick and thin dashed lines indicate the paramagnetic line and the field of the magnetization jump to the 1/8-plateau, respectively. The dotted line is an eye-guide for the signal B. The inset shows the schematic energy level of an isolated $S = 1/2$ antiferromagnetic dimer. $S_{GS} = 0$ is the singlet ground state. For others, see text.

corresponds to the creation of a new triplet into a super-lattice structure at a plateau.[36] Momoi and Totuska proposed that a "supersolid" state appears between the plateaux, in which a spin density wave and superfluid of spins coexist.[13] The latter component gives rise to a gap-less ESR. The present result indicates that a superfluid component (gap-less mode) is also significant at 1/4-plateau and that the plateau is not completely static at 1.6 K. Recently, the static super lattice structure is found by NMR in the 1/8-plateau at 30 mK.[38] For 1/4-plateau, a static super structure may also appear if we measure in much lower temperature below 1.6 K. This point remains for further experimental investigations.

Although the behavior of M is rather conventional, B shows unusual features: (1) location above the paramagnetic line, (2) non-linear field dependence, and (3) disappearance at the jump to the 1/8-plateau. Considering these features, we propose two possible origins of B: (a) AFMR, (b) transition $S_z = 1 \rightarrow S_z = 0$ in the lowest triplets. First we discuss the possibility of AFMR. In AFMR, a deviation from the paramagnetic line is caused by anisotropy and thus the deviation should change for different field orientation. However, the deviation of B is nearly equal between $\boldsymbol{B} \parallel c$ and $\boldsymbol{B} \parallel a$. The most fundamental difficulty of the interpretation by AFMR is that no evidence of 3D-ordering is found below the 1/8-plateau. Actually, in NMR measurement, no static internal field is found in this field range, which shows non-existence of 3D-order.[38]

Next we discuss the possibility of the case (b). In the most simple picture of a isolated dimer system, the $S_z = 1$ level is below the singlet ground state above H_c as shown in the inset of Fig. 11. The transition $S_z = 1 \rightarrow S_z = 0$ shown by the arrow (ν_2) represents ESR of a disordered magnetic state and the resonance field is identical with that of a paramagnetic resonance. In the present system, the level scheme is modified for the anti-level-crossing as shown by the dotted lines. The transition $S_z = 1 \rightarrow S_z = 0$ also changes to that of the dashed arrow (ν_1). The signal B may be assigned as this transition ν_1. Qualitatively, the features (1) and (2) mentioned above are consistent with this interpretation. The strong intensity of B is also consistent with this picture because it is the allowed transition from the ground state. However, a quantitative agreement is difficult with the simple model shown in the inset. In this case, the relation $\nu_1 = \nu_2 + \nu_3$ should hold at each field, where ν_3 is the transition $S_{GS} = 0 \rightarrow S_z = 1$ (note that arrows in the inset are shifted to prevent the overlapping). It is because of the anti-symmetry of the anti-level-crossing around the H_c. However, this relation is not found among O_1, O_2 and B as can be seen clearly in Figs. 4(a) and 4(b). For example while the deviation of B is rather independent of the field direction, O_1 and O_2 are anisotropic. As shown above, the model (b) cannot explain perfectly the behavior of the signal B. We may consider that the nature of the state below the 1/8-plateau seems to be unconventional, which requires further microscopic investigations by using different types of probes.

6. Summary

To be summarized, the following important features are found.

(1) Difference of the symmetry between the nearly degenerated one-triplet excitations O_1 and O_2 are found in the field dependences and in the anti-level-crossing.
(2) Two-singlet bound states are found by the anti-level-crossing with the one-triplet excitation. The one of those is located below the spin gap of the one-triplet, which indicates the proximity to the quantum critical point.
(3) Several triplet bound states are found. The zero field energy gaps are all below the two-particle continuum threshold.
(4) The gap of the lowest quintet$_{BS}$ is below the two-particle continuum threshold; hence it crosses with the one-triplet excitation before the closing of the one-triplet spin gap. Some of the quintet$_{BS}$ modes are assigned as a three-triplet bound state.
(5) The finite magnetization appearing below the 1/8-plateau contains various types of magnetic components caused by the anisotropic mixing.
(6) Two models are proposed for the unusual ESR mode B observed below the 1/8-plateau.
(7) The domination of gap-less ESR signal M indicates that the 1/4-plateau is rather soft compared to the 1/3-plateau.
(8) Qualitative interpretation is made for the selection rules in the one-triplet excitation by considering intra-dimer DM-interaction, inter-dimer DM-interaction and a staggered field.

The present work exhibits various novel features of higher order multiple-particle excitations in a quantum spin gap system.

Acknowledgements

The authors would like to thank T. Sakai, T, Ziman, O. Cépas, K. Totsuka and Y. Fukumoto for valuable discussions. This work was partly supported by a Grant-in-Aid for

Scientific Research on Priority Areas from the Ministry of Education, Culture, Sports, Science and Technology.

1) T. M. Rice: Z. Phys. B **103** (1997) 618.
2) R. W. Smith and D. A. Keszler: J. Solid State Chem. **93** (1991) 430.
3) H. Kageyama, K. Yoshimura, R. Stern, N. V. Mushnikov, K. Onizuka, M. Kato, K. Kosuge, C. P. Slichter, T. Goto and Y. Ueda: Phys. Rev. Lett. **82** (1999) 3168.
4) B. S. Shastry and B. Sutherland: Physica B **108** (1981) 1069.
5) S. Miyahara and K. Ueda: Phys. Rev. Lett. **82** (1999) 3701.
6) Z. Weihong, C. J. Hamer and J. Oitmaa: Phys. Rev. B **60** (1999) 6608.
7) H. Kageyama, M. Nishi, N. Aso, K. Onizuka, T. Yoshihama, K. Nukui, K. Kodama, K. Kakurai and Y. Ueda: Phys. Rev. Lett. **84** (2000) 5876.
8) P. Lemmens, M. Grove, M. Fisher, G. Güntherodt, V. N. Kotov, H. Kageyama, K. Onizuka and Y. Ueda: Phys. Rev. Lett. **85** (2000) 2605.
9) H. Nojiri, H. Kageyama, K. Onizuka, Y. Ueda and M. Motokawa: J. Phys. Soc. Jpn. **68** (1999) 2906.
10) C. Knetter, A. Buehler, E. M. Hartmann and G. Uhrig: Phys. Rev. Lett. **85** (2000) 3958.
11) T. Momoi and K. Totsuka: Phys. Rev. B **61** (2000) 3231.
12) T. Room, U. Nagel, E. Lippmaa, H. Kageyama, K. Onizuka and Y. Ueda: Phys. Rev. B. **61** (2000) 14342.
13) T. Momoi and K. Totsuka: Phys. Rev. B **62** (2000) 15067.
14) Y. Fukumoto: J. Phys. Soc. Jpn. **69** (2000) 2755.
15) H. Nojiri, K. Onizuka, Y. Ueda, T. Asano, Y. Ajiro and M. Motokawa: *Proc. Int. Workshop on Magnetic Excitations in Strongly Correlated Electrons*, J. Phys. Soc. Jpn. **69** (2000) Suppl. B, p. 83.
16) O. Cépas, K. Kakurai, L. P. Regnault, T. Ziman, J. P. Boucher, N. Aso, M. Nishi, H. Kageyama and Y. Ueda: Phys. Rev. Lett. **87** (2001) 167205.
17) S. Miyahara and K. Ueda: cf. ref. 15 J. Phys. Soc. Jpn. **69** (2000) Suppl. B, p. 72.
18) A. Koga and N. Kawakami: Phys. Rev. Lett. **84** (2000) 4461.
19) H. Kageyama, K. Onizuka, T. Yamauchi, Y. Ueda, S. Hane, H. Mitamura, T. Goto, K. Yoshimura and K. Kosuge: J. Phys. Soc. Jpn. **68** (1999) 1821.
20) K. Onizuka, H. Kageyama, Y. Narumi, K. Kindo, Y. Ueda and T. Goto: J. Phys. Soc. Jpn. **69** (1999) 1016.
21) H. Nojiri, H. Ohta, S. Okubo, O. Fujita, J. Akimitsu and M. Motokawa: J. Phys. Soc. Jpn. **68** (1999) 3417.
22) H. Nojiri, S. Luther, M. Motokawa, M. Isobe and Y. Ueda: J. Phys. Soc. Jpn. **69** (2000) 2291.
23) B. Kurniawan, H. Tanaka, K. Takatsu, W. Shiramura, T. Fukuda, H. Nojiri and M. Motokawa: Phys. Rev. Lett. **82** (1999) 1281.
24) T. Asano, H. Nojiri, Y. Inagaki, J. P. Boucher, T. Sakon, Y. Ajiro and M. Motokawa: Phys. Rev. Lett. **84** (2000) 5880.
25) H. Nojiri: *EPR in 21st Century: bases and applications to material-, life-, and earth-sciences*, ed. A. Kawamori, J. Yamauchi and H. Ohta (Elsevier, 2002).
26) H. Kageyama, K. Onizuka, T. Yamauchi and Y. Ueda: J. Cryst. Growth **206** (1999) 65.
27) T. Sakai, O. Cépas and T. Ziman: J. Phys. Soc. Jpn. **69** (2000) 3521.
28) O. Cépas and T. Ziman: *Quantum Properties of Low-Dimensional Antiferromagnets*, ed. Y. Ajiro and J. P. Boucher (Kyushu University Press).
29) O. Cépas, T. Sakai and T. Ziman: Prog. Theor. Phys. Suppl. No. 145 (2002) 43.
30) K. Kakurai, N. Aso, K. Nukui, M. Nishi, H. Kageyama, Y. Ueda, H. Kadowaki and O. Cépas: *Quantum Properties of Low-Dimensional Antiferromagnets*, ed. Y. Ajiro and J. P. Boucher (Kyushu University Press).
31) T. Sakai and H. Shiba: J. Phys. Soc. Jpn. **63** (1994) 867.
32) T. A. Kaplan: Z. Phys. B **49** (1983) 313.
33) L. Shekhtman, O. Entin-Wohlman and A. Aharony: Phys. Rev. Lett. **69** (1992) 836.
34) H. Nojiri, T. Asano, Y. Ajiro, H. Kageyama, Y. Ueda and M. Motokawa: Physica B **294–295** (2001) 14.
35) K. Totsuka, S. Miyahara and K. Ueda: Phys. Rev. Lett. **86** (2001) 520.
36) S. Kimura, S. Hirai, Y. Narumi, K. Kindo, H. Nojiri, H. Kageyama, K. Onizuka and Y. Ueda: Physica B **294–295** (2001) 68.
37) H. Nojiri, H. Kageyama, Y. Ueda and M. Motokawa: J. Magn. Magn. Matter. **226–230** (2001) 1101.
38) K. Kodama, M. Takigawa, M. Horovatic, C. Berthier, H. Kageyama, Y. Ueda, S. Miyahara, F. Becca and F. Mila: Science **298** (2002) 395.
39) M. Oshikawa and I. Affleck: Phys. Rev. Lett. **82** (1999) 5136.